Activation of the P2RX7/IL-18 pathway in immune cells inhibits lung fibrosis

Serena Janho dit Hreich[1,2], Thierry Juhel[1], Sylvie Leroy[2,3,4], Alina Ghinet[5,6,7], Frederic Brau[3], Véronique Hofman[1,2,8,9], Paul Hofman[1,2,8,9], Valérie Vouret-Craviari[1,2]

1. Université Côte d'Azur, CNRS, INSERM, IRCAN, 06108 Nice, France
2. FHU OncoAge, Nice, France
3. Université Côte d'Azur, CNRS, Institut Pharmacologie Moléculaire et Cellulaire, Sophia-Antipolis, France.
4. Université Côte d'Azur, Centre Hospitalier Universitaire de Nice, Pneumology Department, Nice, France
5. Inserm U995, LIRIC, Université de Lille, CHRU de Lille, Faculté de médecine – Pôle recherche, Place Verdun, F-59045 Lille Cedex, France
6. Hautes Etudes d'Ingénieur (HEI), JUNIA Hauts-de-France, UCLille, Laboratoire de chimie durable et santé, 13 rue de Toul, F-59046 Lille, France
7. 'Al. I. Cuza' University of Iasi, Faculty of Chemistry, Bd. Carol I, nr. 11, 700506 Iasi, Romania
8. Laboratory of Clinical and Experimental Pathology and Biobank, Pasteur Hospital, Nice, France
9. Hospital-Related Biobank (BB-0033-00025), Pasteur Hospital, Nice, France

Corresponding author: Valérie VOURET-CRAVIARI

IRCAN, 28 Avenue de Valombrose, 06108 Nice, France.

00 33 (0)492031223

valerie.vouret@univ-cotedazur.fr

Conflict-of-interest statement:

The authors have declared that no conflict of interest exists

ABSTRACT

Idiopathic pulmonary fibrosis (IPF) is an aggressive interstitial lung disease associated with progressive and irreversible deterioration of respiratory functions that lacks curative therapies. It is characterized by destruction of lung architecture due to accumulation of fibroblasts and extracellular matrix proteins, that are the main targets of current antifibrotic therapies. IPF is also associated with a dysregulated immune response, which its importance in IPF is still under debate. P2RX7 is an immunomodulator shown to favor IFN-γ production by immune cells, which is described to be antifibrotic. P2RX7 is expressed and active in IPF and we sought here to determine the ability of P2RX7 in limiting the progression of pulmonary fibrosis. We show that the *P2RX7/IL-18/IFNG* axis is downregulated in IPF patients. Activation of the P2RX7/NLRP3/IL-18 axis in immune cells limits lung fibrosis progression in a mouse model by favoring an anti-fibrotic immune environment, with notably enhanced IFN-γ production by lung T cells. Overall, we show the ability of the immune system to limit lung fibrosis progression by targeting the immunomodulator P2RX7. We also highlight the importance of IL-18 as a key regulator of pulmonary fibrosis and propose that high levels of active IL-18 may represent a better prognosis for IPF patients.

Introduction

Idiopathic pulmonary fibrosis (IPF) is an aggressive interstitial lung disease associated with progressive deterioration of respiratory function that is ultimately fatal. It is characterized by destruction of the lung architecture due to accumulation of fibroblasts and extracellular matrix proteins, resulting in increased lung stiffness and impaired normal breathing.

Pirfenidone and nintedanib have been FDA approved for the treatment of IPF since 2014. They target respectively the key fibrotic cytokine TGFβ and several receptor tyrosine kinases, thereby affecting fibroblast activation and extracellular matrix protein production (1). However, they only slow down the progression of the disease, so new therapeutic strategies and targets are needed.

Fibrosis is also associated with inflammation. In fact, fibrosis is an excessive wound healing and tissue remodeling process due to repeated epithelial injuries releasing damage-associated molecular patterns (DAMPs) that trigger both the adaptive and innate immune systems. Although inflammation has not been considered a target in IPF, due to unsuccessful initial clinical trials of anti-inflammatory drugs (2) or cyclophosphamide during exacerbations (3), growing evidence suggest that altering specific immune populations that promote or attenuate disease progression may be beneficial (4).

Extracellular adenosine triphosphate (eATP) is a DAMP, released in high concentrations from injured cells in IPF patients. High levels of eATP are recognized by the P2X7 receptor (P2RX7) and are both required for the establishment of the bleomycin lung fibrosis mouse model (5). Activation of P2RX7 induces the opening of macropores, resulting in cell death (6), but also leads to the assembly of the NLRP3 inflammasome and the release of mature IL-1β and IL-18 (7). Consequently, P2RX7 has the ability to trigger an immune response.

IL-1β is a proinflammatory cytokine with high profibrotic properties, as it promotes collagen deposition through IL-17A and TGFβ production(8–10) but also promotes the activation and recruitment of inflammatory cells such as eosinophils and neutrophils. Indeed, deficiency of IL-1βR or its blockade ameliorate experimental fibrosis (11–13). In contrast, the role of IL-18 is not clear. Indeed, conflicting

experimental studies show that IL-18 could either promote (14) or attenuate (15) fibrosis. However, high levels of IL-18BP, a natural antagonist of IL-18, are associated with reduced overall survival in IPF patients (16), suggesting that the activity of IL-18 may be required for improved survival.

IL-18 was originally described as IFN-γ-inducing factor (IGIF) and therefore boosts IFN-γ production by T cells and NK cells (17). Not only has IFN-γ antiproliferative properties (18) but it also inhibits TGFβ activity (19, 20) and therefore inhibits fibroblast activation and differentiation into myofibroblasts, alleviates TGFβ-mediated immunosuppression, inhibits extracellular matrix accumulation and collagen production (21–24) and thus promotes an antifibrotic immune microenvironment, making IFN-γ a cytokine with antifibrotic properties. However, parenteral systemic administration of IFN-γ failed in clinical trials (INSPIRE; NCT 00075998) (25), whereas local administration by inhalation showed promising results (26–30).

One way to increase IFN-γ production locally and selectively in the lung would be to alter the phenotype of T cells since the polarization of T lymphocytes has been shown to impact fibroblasts' fate and immune infiltrate (4, 31). Indeed, T cells have been recently shown to selectively kill myofibroblasts through IFN-γ release and limit the progression of lung and liver fibrosis in preclinical models (32) and set up an immune memory in the long term since IFN-γ-producing tissue resident memory T cells protect against fibrosis progression (33), highlighting the importance IFN-γ producing T cells in this disease. Accordingly, $CD4^+$-producing IFN-γ T cells are decreased in IPF and correlate with a better prognosis in IPF patients (31, 34, 35).

Given the ability of IL-18 to shape the phenotype of T cells by inducing IFN-γ, we proposed to increase local IFN-γ production via the P2RX7/IL-18 axis as a therapeutic strategy in pulmonary fibrosis. We chose to use a P2RX7-specific positive modulator, which we synthesized, to enhance the activities of P2RX7, particularly IL-18, only in the presence of high eATP (36).

Results

Expression of P2RX7 and IL-18 activity are dampened in IPF patients

The canonical release of IL-18 is due to activation of the P2RX7/NLRP3 pathway (7). Since high levels of eATP are found in IPF patients (5) and P2RX7 is activated by such levels, it was of particular interest to investigate the involvement of P2RX7 in this disease. We used a publicly available dataset of lung homogenates from control and IPF patients (GSE47460). We found that the expression of P2RX7 is downregulated in IPF patients (Figure 1A and B), as well as the components of the NLRP3 inflammasome (Supplemental Figure 1). Since IL-18 is constitutively expressed (37), which partly explains the lack of difference between control and IPF patients (Figure 1B), we investigated the signaling pathway downstream of IL-18. IL-18 binds to its receptor IL-18R1 coupled to its adaptor protein IL-18RAP which is required for IL-18 signaling and IFN-γ expression. We show that IL-18R1, IL-18RAP and IFN-γ (Figure 1B) are downregulated in IPF patients. Moreover, the expression of P2RX7 and IL-18 signaling (IL-18 and IL-18RAP) correlates with the IFN-γ response as well as with the modulation of the immune response in IPF patients (Figure 1C, Supplemental Figure 1B). These results highlight that the P2RX7/IL-18 signaling pathway is dampened and that this pathway is able to modulate the immune response in IPF patients.

Activation of P2RX7 inhibits the onset of pulmonary fibrosis in the bleomycin mouse model

In order to boost the P2RX7/IL-18 signaling, we chose a positive modulator of P2RX7 called HEI3090, which enhances its activity only in the presence of high eATP levels as we have previously shown (36). High eATP levels are found in fibrotic lungs, in IPF patients as well as in the bleomycin (BLM) mouse model of pulmonary fibrosis that we used to test the antifibrotic potential of HEI3090. Activation of P2RX7 with HEI3090 (Figure 2A) reduced the development of pulmonary fibrosis, as evidenced by less thickening of alveolar walls and free air space (Figure 2B), as assessed by the fibrosis score (Figure 2C). Accumulation of extracellular matrix proteins is a hallmark of fibrosis. Therefore, collagen content was assessed by polarized light microscopy on lung sections stained with Sirius red. We show that collagen

content was reduced in lungs of HEI3090-treated mice (Figure 2B and D). We also weighed the lungs of the mice at the end of the experiment and show that the lung weight of HEI3090-treated mice decreased compared with control mice (Figure 2E), indicating less fibrosis and inflammation. In addition, activation of P2RX7 with HEI3090 increased the release of IL-18 in the sera of the mice (Figure 2F), as well as the production of IFN-γ by lung T cells (Figure 2G). This increase in IFN-γ production is only seen in CD3+ T cells and not in overall lung immune cells or in other subsets of lymphocytes (Supplemental Figure 2). These results show that HEI3090 inhibits the onset of lung fibrosis when given during the acute inflammation phase, mimicking the exacerbation episodes in IPF patients (38), through boosting the P2RX7/IL-18/IFN-γ pathway.

It was also important to test the antifibrotic potential of HEI3090 in mice with an established fibrosis. Indeed, administration of HEI3090 in the fibrotic phase of the BLM mouse model also inhibited pulmonary fibrosis' progression given the reduced fibrosis score and collagen content in lungs of HEI3090-treated mice (Supplemental Figure 2A-C).

Overall, these results show that enhancing the activation of P2RX7 with a positive modulator reduces lung fibrosis and increases the release of IL-18 and IFN-γ.

HEI3090 requires the P2RX7/NLRP3/IL-18 pathway in immune cells to inhibit lung fibrosis

We wanted to further investigate the mechanism of action of HEI3090 by identifying the cellular compartment and signaling pathway required for its activity. Since the expression of P2RX7 and the P2RX7-dependent release of IL-18 are mostly associated with immune cells(39), we investigated whether immune cells were required for the antifibrotic effect of HEI3090.

To do so, we performed an adoptive transfer experiment with WT P2RX7-expressing splenocytes (Figure 3A, supplemental Figure 5E) into *p2rx7*$^{-/-}$ mice one day before BLM administration. We show that restriction of P2RX7 expression on immune cells restored the antifibrotic effect of HEI3090 based on the architecture of the lung: lungs of HEI3090-treated mice show more free airspace and thinner alveolar walls (Figure 3B), as well as an overall lower fibrosis score (Figure 3C) than control lungs.

Moreover, HEI3090 activity requires P2RX7 expression, as this effect was lost in *p2rx7*$^{-/-}$ mice (Supplemental Figure 5A and B) (36). Since the bleomycin mouse model relies on P2RX7-expressing epithelial cells (5), we wanted to validate further the role of P2RX7-expressing immune cells in a mouse model where P2RX7 is expressed by non-immune cells. To do so, we reduced the expression of P2RX7 and its activity by repeated i.v. administration of *p2rx7*$^{-/-}$ splenocytes in WT mice (Supplemental Figure 4). In this setting, HEI3090 was unable to limit the progression of fibrosis. This highlights the important role of immune cells and rules out a major role of non-immune P2RX7-expressing cells, such as fibroblasts, in the antifibrotic effect of HEI3090.

To test the importance of the NLRP3/IL-18 pathway downstream of P2RX7, we performed an adoptive transfer of *nlrp3*$^{-/-}$ and *il18*$^{-/-}$ splenocytes into *p2rx7*$^{-/-}$ mice, expressing similar levels of P2RX7 as WT splenocytes (Supplemental Figure 5E), but also the same levels of IL-18 and NLRP3 (Supplemental Figure 5F). The absence of NLRP3 and IL-18 in P2RX7-expressing immune cells abrogated the ability of HEI3090 to inhibit lung fibrosis because the lung architecture resembled that of control mice (Figure 3D-G). Activation of the P2RX7/NLRP3 pathway is generally associated with pro-inflammatory and pro-fibrotic IL-1β release. IL-1β however, was not involved in the antifibrotic effect of HEI3090 (Supplemental Figure 5C), nor were its levels affected by HEI3090 in WT mice (Supplemental Figure 5D).

Overall, the P2RX7/NLRP3/IL-18 axis in immune cells is required to limit lung fibrosis progression, highlighting the efficacy in targeting the immune system in this disease.

HEI3090 shapes immune cell infiltration in the lungs

We have shown this far the ability of the immune P2RX7/IL-18 axis to limit lung fibrosis progression as well as the ability of HEI3090 to enhance the release of IL-18 and IFN-γ. We next investigated if HEI3090 had another impact on the immune composition of the lung. Although levels of CD3+ T cells and T cell subsets were unchanged (Supplemental Figure 6A and B), including the profibrotic Th17 cells (Figure 4A), IL-17A production by Th17 cells is markedly attenuated after HEI3090 treatment (Figure 4A),

consistent with the ability of IFN-γ to inhibit IL-17A production (40). Considering the strong profibrotic properties of TGFβ and its mutual antagonism with IFN-γ (41, 42), we checked whether HEI3090 had an effect on TGFβ levels. Indeed, treatment with HEI3090 reduced TGFβ-producing immune cells in the lung as well as TGFβ production (Figure 4B). Notably, HEI3090 treatment reduced TGFβ production in NK cells but not in T-cell subsets (Supplemental Figure 6C).

Pulmonary fibrosis is also favored and driven by the recruitment of inflammatory cells, mainly from the myeloid lineage. Monocytes are highly inflammatory cells that are recruited to the lung and differentiate into alveolar macrophages, both of which have strong profibrotic properties (43–45). We demonstrated that in HEI3090-treated mice, the number of inflammatory monocytes decreased markedly (Figure 4C), whereas the number of alveolar macrophages remained unchanged (Figure 4D), consistent with the prognostic ability of monocyte count in IPF progression (46–49). We also examined other inflammatory cells with profibrotic properties, such as eosinophils (50) that are less present in HEI3090-treated lungs (Figure 4E), or PMN levels that remain unchanged by HEI3090 treatment (Supplemental Figure 6A).

Interestingly, activation of P2RX7 with HEI3090 mainly affected immune populations in the lungs, as no significant change in cell populations was observed in the spleens of mice (Supplemental Figure 6D). However, HEI3090 reactivated an immune response with higher levels of dendritic cells and lymphocytes in the spleens of therapeutically treated mice (Supplemental Figure 2E).

These results show that activation of P2RX7 with HEI3090 promotes an antifibrotic cytokinic profile in lung immune cells and attenuates lung inflammation.

Evaluation of IL-18 bioavailability is a promising tool to predict outcome in IPF patients

Given that IL-18 is required for the antifibrotic effect of HEI3090, we wondered whether IL-18 could predict the outcome of IPF patients. To this extent, we analyzed the IL-18 levels of 9 healthy controls and 18 IPF patients in plasma samples collected before the start of treatment (Table 1). Since IL-18 has a higher affinity for IL-18BP than for its receptor and commercially available ELISAs do not detect only

free IL-18, we were particularly interested in investigating the levels of free, active IL-18 as well as neutralized, inactive IL-18 (IL-18/ IL-18BP complex).

We show that the bioavailability of IL-18 (i.e., the levels of free IL-18 and complexed IL-18) as well as total levels of IL-18 are increased in IPF patients compared with healthy subjects (Figure 5A, Supplemental Figure 7A), whereas the levels of the antagonist IL-18BP are unchanged (Supplemental Figure 7A). Looking at the overall survival of these patients, high levels of free IL-18 seem to predict better outcome of IPF patients (Figure 5C), whereas this is not true for levels of complexed IL-18. However, due to the small number of patients in our cohort, this result should be confirmed on a larger scale.

These results suggest the possible benefit of an active IL-18 in the pathophysiology of pulmonary fibrosis and warrant analysis of free IL-18 as a promising biomarker for predicting outcome in IPF patients.

Discussion

A major unmet need in the field of IPF is new treatment to fight this uncurable disease. In this study, we demonstrate the ability of immune cells to limit lung fibrosis progression. Based on the hypothesis that a local activation of a T cell immune response and upregulation of IFN-γ production has antifibrotic proprieties, we used the HEI3090 positive modulator of the purinergic receptor P2RX7, previously developed in our laboratory (36), to demonstrate that activation of the P2RX7/IL-18 pathway inhibits lung fibrosis in the bleomycin mouse model.

We have demonstrated that lung fibrosis progression is inhibited by HEI3090 in the acute but also in the fibrotic phase of the BLM fibrosis mouse model, i.e. during the period of fibroproliferation. This lung fibrosis mouse model is classically used in preclinical studies and has been designated recently as the best model for IPF (51). The efficacy of HEI3090 to inhibit lung fibrosis was evaluated histologically using the Ashcroft score (scaled from 0 to 8) where lung architecture and alveolar septa are studied (52). In both settings, HEI3090 reduced alveolar wall thickness and accumulation of collagen fibers, but also reduced the weight of the lungs. Altogether, these criteria highlight a comprehensive pre-clinical evaluation of HEI3090 as a new anti-fibrotic therapy.

Our study showed that inhibition of fibrosis development by HEI3090 was associated with an increased release of IL-18, accompanied by increased production of IFN-γ by lung T cells. P2RX7 is expressed by various immune and non-immune cells, but its expression is the highest in dendritic cells (DCs) and macrophages (53), from which IL-18 is mainly released to shape the T-cell response (54) and increase T-cell IFN-γ production (55). Collectively, and consistent with the immunomodulatory properties of P2RX7, these observations suggest that HEI3090 may target P2RX7-expressing antigen-presenting cells to influence the T-cell response, which may explain the selective T-cell increase in IFN-γ in HEI3090-treated mice. Accordingly, we have previously shown that HEI3090 targets the P2RX7/IL-18 axis in DCs to shape the immune response in a lung tumor mouse model (36).

Activation of P2RX7 with HEI3090 not only increased IFN-γ production by T cells but it also reshaped the immune and cytokinic composition of the lung. Indeed, lungs of HEI3090-treated mice show a decrease in IL-17A production by Th17 cells and TGFβ production by lung immune cells. Moreover, lung inflammation is dampened after HEI3090 treatment, since the number of inflammatory monocytes and eosinophils decreases. It is not known whether this cytokinic and anti-inflammatory switch is solely due to the IL-17A and TGFβ-suppressive property of IFN-γ (56–58), or whether it is a combination with the cell death-inducing property of P2RX7 (6).

The novelty of this approach is that it targets and alters the immune environment of the lung. Indeed, the use of a P2RX7-specific modulator that acts only in an ATP-rich environment was effective in promoting an anti-inflammatory and anti-fibrotic phenotype by altering several key mediators of disease. In contrast to current therapies (59), no side effects were observed when mice were treated with HEI3090, further supporting this targeted approach. Furthermore, since current therapies and HEI3090 have different mechanisms of action, the combination of these therapies could have additive or synergistic effects. It is also important to note that our strategy is unconventional, as P2RX7 is known to be pro-inflammatory through IL-1β-release. However, HEI3090 was unable to increase IL-1β release *in vivo* in this model, even though it efficiently increased IL-18 release. This observation is consistent with our previous *in vivo* and *in vitro* studies (36), allowing us to rule out the pro-inflammatory and pro-fibrotic effects of P2RX7-dependent IL-1β release. Consistent with this finding, it has been reported that ATP stimulation of alveolar macrophages derived from both IPF and lung cancer patients resulted only in an increase in IL-18 (60, 61), which was explained by an impaired NLRP3 inflammasome and a defective autophagy described in IPF patients (62). Interestingly, autophagy can be regulated by P2RX7 (63) and is one of the pathways that allow the release of IL-1β from the cell (64). Moreover, unlike IL-1β, IL-18 is constitutively expressed in human and mouse immune cells (37) but also in non-immune cells such as fibroblasts (65) and lung epithelium (66) and is both matured and released after NLRP3 activation. Therefore, it is currently not known whether the lack of IL-1β release is due to the different

cytokine expression pattern or whether there is IL-1β-specific regulation following an enhanced activation of P2RX7 or a defective NLRP3 inflammasome.

In this study, we emphasize the importance of IL-18 for an antifibrotic effect. Several studies have indicated that P2RX7/NLRP3/IL-18 promote disease progression using knock out mice or inhibitors (5, 14, 65). However, experimental mouse models rely on lung epithelial cell injury that has been shown to activate the NLRP3 inflammasome in the lung epithelium as a first step (5, 12) and release danger signals that activate the immune system as a second step. Therefore, initial lung injury to epithelial cells is reduced or absent in *p2rx7*$^{-/-}$ and *nlrp3*$^{-/-}$ mice, indicating that P2RX7 and NLRP3 are required for the establishment of the bleomycin mouse model rather than their role in an already established fibrosis, which has not yet been studied. In addition, NLRP3 and the release of IL-1β and IL-18 from fibroblasts have been shown to promote myofibroblast differentiation and extracellular matrix production (65, 67, 68). These observations suggest that fibrosis mouse models initially rely on NLRP3 activation by nonimmune cells and encourage further studies on the contribution of the NLRP3 inflammasome in immune cells to fibrosis progression *in vivo*. We have shown that the NLRP3 pathway is downregulated in IPF patients (Supplemental Figure1), whereas plasmatic IL-18 is increased (Figure 5). It is important to note that these two results cannot be compared because NLRP3 and IL-18 levels are measured in bulk in lung tissue versus plasma, respectively. Moreover, NLRP3 activity cannot be assessed at the mRNA level because its activation relies on protein assembly and sequential cleavages. Since we have highlighted the importance of this pathway in immune cells for delaying fibrosis progression, we propose that IL-18 may have different effects depending on the cell type.

We also showed that expression of the P2RX7/IL-18/IFN-γ pathway is attenuated in IPF patients where TGFβ levels are high (69), consistent with the ability of TGFβ to downregulate IL-18R expression and IL-18-mediated IFN-γ production (70). These results confirm the beneficial effects of enhancing activation of the P2RX7/IL-18/IFN-γ pathway.

Beside an urgent need of new treatments for IPF, there is also a lack of biomarkers, such as prognostic biomarkers, markers of disease activity, or markers of drug efficacy. We show here that the levels of free plasmatic IL-18 have the potential to be an indicator of patient survival by determining, for the first time in IPF, the concentrations of free and complexed IL-18. Indeed, most human studies measure the total amount of IL-18 without considering its binding to IL-18BP and the free active amount of the cytokine. Our results indicate that the state of IL-18 in patients' plasma is promising in predicting disease progression. However, it is imperative to further validate the predictive value for the broader IPF population with a larger patient cohort before adopting IL-18 for clinical use. In addition, determination of IL-18 levels in patients' bronchoalveolar lavage fluid could more accurately represent lungs levels of IL-18. Given the potential effects of pirfenidone and nintedanib on IL-18 levels in preclinical models (71–73), determining IL-18 shifts during treatment would be highly interesting to evaluate potential changes in patients' outcome and to examine IL-18 levels as a companion test of treatment efficacy.

Overall, we highlight in this study the ability of the P2RX7/NLRP3/IL-18 pathway in immune cells to inhibit the onset of lung fibrosis by using a positive modulator of P2RX7 that acts selectively in an eATP-rich environment such as fibrotic lung. The unique feature of this strategy is that it enhances the antifibrotic and it attenuates the pro-fibrotic properties of immune cells, with no reported side effects. In addition, we show that active IL-18 can predict better patient outcome, which may be helpful in the long run for patient treatment strategy and subsequent introduction of pipeline drugs (74).

Methods

Patients

We conducted a retrospective study on patients harboring idiopathic pulmonary fibrosis (75) enrolled at the Nice University Hospital since 2014. Before analysis, all samples were stored in the biobank of the Nice University Hospital, France (BB-0033-00025) approved by French Government. Written informed consent was obtained from each participant. The clinical database COLIBRI linked to the biobank was authorized by the French Data Protection Authority (CNIL authorization number #DR-2018-094) and the French ethical research committee (CPP reference number #2017 AO266251). Clinical characteristics are listed in table 1. Progressive IPF was defined as at least two of three criteria (Worsened respiratory symptoms, increased extent of fibrotic changes on chest imaging, and absolute decline in FVC ≥10% predicted or in DLCO ⩾10%) occurring within one year of biobanking with no alternative diagnosis.

Free IL-18 measurement in plasma of patients

Levels of total IL-18, IL-18BP and IL-18/IL-18BP complex were determined by human DuoSet ELISA kits from R&D systems according to manufacturer's instructions. The law of mass action was used to calculate the level of free IL-18. Single IL-18BP molecule binds a single molecule of IL-18, with a dissociation constant (Kd) of 400 pM. Therefore, the level of free IL-18 was calculated from the equation (76) $x = \frac{-b+\sqrt{b^2-4c}}{2}$ where: x = [IL-18free], b = [IL-18BP] – [IL-18] + Kd, and c = -Kd × [IL-18]

Microarray

mRNA expression profile was obtained from Gene Expression Omnibus (GEO) database (GSE47460) using the GPL14550. Microarray was done on whole lung homogenate from subjects undergoing thoracic surgery from healthy subjects with no lung-related pathology or from subjects diagnosed as having interstitial lung disease as determined by clinical history, CT scan, and surgical pathology.

Expression profile belong to the Lung Tissue Research Consortium (LTRC). 122 patients with UIP/IPF and 91 healthy controls were analyzed in this study.

Mice

Mice were housed under standardized light–dark cycles in a temperature-controlled air-conditioned environment under specific pathogen-free conditions at IRCAN, Nice, France, with free access to food and water. All mouse studies were approved by the committee for Research and Ethics of the local authorities (CIEPAL #598, protocol number APAFIS 21052-2019060610506376) and followed the European directive 2010/63/UE, in agreement with the ARRIVE guidelines. Experiments were performed in accord with animal protection representative at IRCAN. *p2rx7*$^{-/-}$ (B6.129P2-P2rx7tm1Gab/J) are from the Jackson Laboratory. C57BL/6J OlaHsD male mice (WT) were supplied from Envigo (Gannat, France).

Induction of lung fibrosis

WT or *p2rx7*$^{-/-}$ male mice (8 weeks) were anesthetized with ketamine (25mg/kg) and xylazine (2.5 mg/kg) under light isoflurane and were given 2.5 U/kg of bleomycin sulfate (Sigma-Aldrich) by intranasal route. Mice were treated i.p. every day with vehicle (PBS, 10% DMSO) or with HEI3090 (1.5 mg/kg in PBS, 10% DMSO) (36) starting D1 or D7 post bleomycin delivery, as mentioned in the figures.

After 14 days of treatment, lungs were either fixed for paraffin embedding or weighted and analyzed by flow cytometry.

Adoptive transfer in *p2rx7* deficient mice

Spleens from C57BL/6J male mice (8-10 weeks) were collected and digested with the spleen dissociation kit (Miltenyi Biotech) according to the supplier's instructions. 3.10^6 splenocytes were injected i.v. in *p2rx7*$^{-/-}$ mice 1 day before intranasal delivery of bleomycin. Mice were treated i.p. every day for 14 days with vehicle (PBS, 10% DMSO) or with HEI3090 (1.5 mg/kg in PBS, 10% DMSO). *Nlrp3*$^{-/-}$ spleens were a kind gift from Dr Laurent Boyer, *il18*$^{-/-}$ spleens from Dr George Birchenough and *il1b*$^{-/-}$ spleens from Dr Bernhard Ryffel, all on a C57BL/6J background.

Histology

Lungs were collected and fixed in 3% formamide for 16 h prior inclusion in paraffin. Lungs sections (3 µm) were stained with hematoxylin & eosin or with Sirius red (Abcam) according to the supplier's instructions. Fibrosis was assessed on whole lungs using the Ashcroft modified method (52).

Levels of collagen on whole lungs were assessed on Sirius Red polarized light images taken with HD - Axio Observer Z1 Microscope ZEISS microscope using ImageJ. The collagen amount given by the polarization intensity of the Sirius red staining of the lung slices was quantified with a homemade ImageJ/Fiji (77) macro program. The mean gray value of the collagen staining was measured in the fibrotic regions excluding the signal coming from vessels and lung epithelia using dedicated masks. The binary masks were obtained after median filtering and manual thresholding, from the transmission images for the fibrotic one and the polarization images for the vessels. The intersection of these masks is then applied on the polarization image to get specifically the mean gray value of fibrotic collagen.

Flow cytometry and antibodies

Lungs or spleens were collected and digested with the lung or spleen dissociation kit (Miltenyi Biotech) according to the supplier's instructions. Red blood cells were lysed using ACK lysis buffer (Gibco). Fc receptors were blocked using anti-CD16/32 (2.4G2) antibodies followed by surface staining by incubating cells on ice, for 20 min, with saturating concentrations of labeled Abs (Supplemental Table 1) in PBS, 5% FBS and 0.5% EDTA. Tregs were identified using the transcription factor staining Buffer Set (eBioscience) for FoxP3 staining. Intracellular staining was performed after stimulation of single-cell suspensions with Phorbol 12-myristate 13-acetate (PMA at 50 ng mL^{-1}, Sigma), ionomycin (0.5 µg mL^{-1}, Sigma) and 1 µL mL^{-1} Golgi Plug™ (BD Biosciences) for 4 h at 37°C 5% CO_2. Cells were incubated with Live/Dead stain (Invitrogen), according to the manufacturer protocol prior to surface staining. Intracellular staining was performed using Cytofix/Cytoperm™ kit (BD biosciences) following the manufacturer's instructions. Samples were acquired on CytoFLEX LX (Beckman Coulter) and analyzed using FlowJo (LLC).

ELISA

Sera of mice were collected at the end of the experiment and stored at −80 °C before cytokine detection by ELISA using mouse IL-1 beta/IL-1F2 (R&D) and IL-18 (MBL) according to the supplier's instructions.

Western Blot

Single cell suspensions of whole lungs were lysed with Laemmli buffer (10% glycerol, 3% SDS, 10 mM Na2HPO4) with protease inhibitor cocktail (Roche). Proteins were separated on a 12% SDS-PAGE gel and electro transferred onto PVDF membranes, which were blocked for 30 min at RT with 3% bovine serum albumin or 5% milk. Membranes were incubated with primary antibodies (see Table 2) diluted at 4 °C overnight. Secondary antibodies (Promega) were incubated for 1 h at RT. Immunoblot detection was achieved by exposure with a chemiluminescence imaging system (PXI Syngene, Ozyme) after membrane incubation with ECL (Immobilon Western, Millipore). The bands intensity values were normalized to that of β-actin using ImageJ software.

Statistical analyses

All analyses were carried out using Prism software (GraphPad). Mouse experiments were performed on at least n = 5 individuals, as indicated. Mice were equally divided for treatments and controls. Data is represented as mean values and error bars represent SEM. Two-tailed Mann–Whitney and unpaired t-test were used to evaluate the statistical significance between groups. For survival analyses, the log-rank Mantel-Cox test was used. For correlation analyses, Spearman test was used for the Gene Set Enrichment Analyses (GSEA)

Study approval

Plasmas used in this study were collected from IPF patients enrolled at the Nice University Hospital (see table 1) in compliance with consent procedures accepted by the French Data Protection Authority (CNIL authorization number #DR-2018-094) and the French ethical research committee (CPP reference number #2017 AO266251).

Mice were handled in accordance with the committee for Research and Ethics of the local authorities (CIEPAL #598, protocol number APAFIS 21052-2019060610506376) and followed the European directive 2010/63/UE.

Authors contribution

S.J.H. and VV-C, conception and design; S.J.H., TJ and VV-C, performed research; S.J.H., SL, PH and VV-C, analysis and interpretation; AG, contributed reagents; SL, VH and PH, contributed tissue specimens; S.J.H. and VV-C, wrote the paper

Acknowledgements

This research was funded by Cancéropôle PACA, the French Government (National Research Agency, ANR through the "Investments for the Future": program reference #ANR-11-LABX-0028-01), SJH is funded by the "Ligue Nationale Contre le Cancer" and the "Fondation pour la recherche medicale" grant number #FDT202106013099 and ARC (grant number ARCTHEM2021020003478). The authors also acknowledge the financial support received from the Executive Unit for Financing Higher Education, Research, Development and Innovation (UEFISCDI), Bucharest, Romania (grant number PN-III-P4-ID-PCE-2020-0818, acronym REPAIR).

The authors wish to thank Dr George Birchenough, Dr Laurent Boyer and Dr Bernhard Ryffel for sharing *il18*$^{-/-}$, *nlrp3*$^{-/-}$ and *il1b*$^{-/-}$ spleens respectively. We thank Jennifer Griffonet and Lorenne Philibert for patient management. Members of the COST PRESTO (CA21130) are acknowledged for their valuable discussion.

References

1. Heukels P, Moor CC, von der Thüsen JH, Wijsenbeek MS, Kool M. Inflammation and immunity in IPF pathogenesis and treatment.. *Respir Med* 2019;147:79–91.

2. Idiopathic Pulmonary Fibrosis Clinical Research Network et al. Prednisone, azathioprine, and N-acetylcysteine for pulmonary fibrosis.. *N Engl J Med* 2012;366(21):1968–77.

3. Naccache J-M et al. Cyclophosphamide added to glucocorticoids in acute exacerbation of idiopathic pulmonary fibrosis (EXAFIP): a randomised, double-blind, placebo-controlled, phase 3 trial. *Lancet Respir Med* 2022;10(1):26–34.

4. Shenderov K, Collins SL, Powell JD, Horton MR. Immune dysregulation as a driver of idiopathic pulmonary fibrosis.. *J Clin Invest* 2021;131(2). doi:10.1172/JCI143226

5. Riteau N et al. Extracellular ATP is a danger signal activating P2X7 receptor in lung inflammation and fibrosis.. *Am J Respir Crit Care Med* 2010;182(6):774–83.

6. Surprenant A, Rassendren F, Kawashima E, North RA, Buell G. The cytolytic P2Z receptor for extracellular ATP identified as a P2X receptor (P2X7).. *Science* 1996;272(5262):735–8.

7. Perregaux DG, McNiff P, Laliberte R, Conklyn M, Gabel CA. ATP acts as an agonist to promote stimulus-induced secretion of IL-1 beta and IL-18 in human blood.. *J Immunol* 2000;165(8):4615–23.

8. Wilson MS et al. Bleomycin and IL-1beta-mediated pulmonary fibrosis is IL-17A dependent.. *J Exp Med* 2010;207(3):535–52.

9. Sutton CE et al. Interleukin-1 and IL-23 induce innate IL-17 production from gammadelta T cells, amplifying Th17 responses and autoimmunity.. *Immunity* 2009;31(2):331–41.

10. Doerner AM, Zuraw BL. TGF-beta1 induced epithelial to mesenchymal transition (EMT) in human bronchial epithelial cells is enhanced by IL-1beta but not abrogated by corticosteroids.. *Respir Res* 2009;10:100.

11. Couillin I et al. IL-1R1/MyD88 signaling is critical for elastase-induced lung inflammation and emphysema.. *J Immunol* 2009;183(12):8195–202.

12. Gasse P et al. Uric acid is a danger signal activating NALP3 inflammasome in lung injury inflammation and fibrosis.. *Am J Respir Crit Care Med* 2009;179(10):903–13.

13. Gasse P et al. IL-1R1/MyD88 signaling and the inflammasome are essential in pulmonary inflammation and fibrosis in mice.. *J Clin Invest* 2007;117(12):3786–99.

14. Zhang L-M et al. Neutralization of IL-18 by IL-18 binding protein ameliorates bleomycin-induced pulmonary fibrosis via inhibition of epithelial-mesenchymal transition.. *Biochem Biophys Res Commun* 2019;508(2):660–666.

15. Nakatani-Okuda A et al. Protection against bleomycin-induced lung injury by IL-18 in mice.. *Am J Physiol Lung Cell Mol Physiol* 2005;289(2):L280-7.

16. Nakanishi Y et al. IL-18 binding protein can be a prognostic biomarker for idiopathic pulmonary fibrosis.. *PLoS One* 2021;16(6):e0252594.

17. Okamura H et al. Cloning of a new cytokine that induces IFN-gamma production by T cells.. *Nature* 1995;378(6552):88–91.

18. Elias JA, Jimenez SA, Freundlich B. Recombinant gamma, alpha, and beta interferon regulation of human lung fibroblast proliferation.. *Am Rev Respir Dis* 1987;135(1):62–5.

19. Ulloa L, Doody J, Massagué J. Inhibition of transforming growth factor-beta/SMAD signalling by the interferon-gamma/STAT pathway.. *Nature* 1999;397(6721):710–3.

20. Varga J et al. Interferon-gamma reverses the stimulation of collagen but not fibronectin gene expression by transforming growth factor-beta in normal human fibroblasts.. *Eur J Clin Invest* 1990;20(5):487–93.

21. Gurujeyalakshmi G, Giri SN. Molecular mechanisms of antifibrotic effect of interferon gamma in bleomycin-mouse model of lung fibrosis: downregulation of TGF-beta and procollagen I and III gene expression.. *Exp Lung Res* 21(5):791–808.

22. Gillery P et al. Gamma-interferon inhibits extracellular matrix synthesis and remodeling in collagen lattice cultures of normal and scleroderma skin fibroblasts.. *Eur J Cell Biol* 1992;57(2):244–53.

23. Duncan MR, Berman B. Gamma interferon is the lymphokine and beta interferon the monokine responsible for inhibition of fibroblast collagen production and late but not early fibroblast proliferation.. *J Exp Med* 1985;162(2):516–27.

24. Yuan W et al. Negative modulation of alpha1(I) procollagen gene expression in human skin fibroblasts: transcriptional inhibition by interferon-gamma.. *J Cell Physiol* 1999;179(1):97–108.

25. King TE et al. Effect of interferon gamma-1b on survival in patients with idiopathic pulmonary fibrosis (INSPIRE): a multicentre, randomised, placebo-controlled trial.. *Lancet* 2009;374(9685):222–8.

26. Diaz KT et al. Delivery and safety of inhaled interferon-γ in idiopathic pulmonary fibrosis.. *J Aerosol Med Pulm Drug Deliv* 2012;25(2):79–87.

27. Smaldone GC. Repurposing of gamma interferon via inhalation delivery.. *Adv Drug Deliv Rev* 2018;133:87–92.

28. Skaria SD, Yang J, Condos R, Smaldone GC. Inhaled Interferon and Diffusion Capacity in Idiopathic Pulmonary Fibrosis (IPF).. *Sarcoidosis Vasc Diffuse Lung Dis* 2015;32(1):37–42.

29. Fusiak T, Smaldone GC, Condos R. Pulmonary Fibrosis Treated with Inhaled Interferon-gamma (IFN-γ).. *J Aerosol Med Pulm Drug Deliv* 2015;28(5):406–10.

30. Prior C, Haslam PL. In vivo levels and in vitro production of interferon-gamma in fibrosing interstitial lung diseases.. *Clin Exp Immunol* 1992;88(2):280–7.

31. Luzina IG, Todd NW, Iacono AT, Atamas SP. Roles of T lymphocytes in pulmonary fibrosis.. *J Leukoc Biol* 2008;83(2):237–44.

32. Sobecki M et al. Vaccination-based immunotherapy to target profibrotic cells in liver and lung.. *Cell Stem Cell* 2022;29(10):1459-1474.e9.

33. Collins SL et al. Vaccinia vaccine–based immunotherapy arrests and reverses established pulmonary fibrosis. *JCI Insight* 2016;1(4). doi:10.1172/jci.insight.83116

34. Xu J, Mora AL, LaVoy J, Brigham KL, Rojas M. Increased bleomycin-induced lung injury in mice deficient in the transcription factor T-bet.. *Am J Physiol Lung Cell Mol Physiol* 2006;291(4):L658-67.

35. Giri SN, Hyde DM, Marafino BJ. Ameliorating effect of murine interferon gamma on bleomycin-induced lung collagen fibrosis in mice.. *Biochem Med Metab Biol* 1986;36(2):194–7.

36. Douguet L et al. A small-molecule P2RX7 activator promotes anti-tumor immune responses and sensitizes lung tumor to immunotherapy.. *Nat Commun* 2021;12(1):653.

37. Puren AJ, Fantuzzi G, Dinarello CA. Gene expression, synthesis, and secretion of interleukin 18 and interleukin 1beta are differentially regulated in human blood mononuclear cells and mouse spleen cells.. *Proc Natl Acad Sci U S A* 1999;96(5):2256–61.

38. Peng R et al. Bleomycin Induces Molecular Changes Directly Relevant to Idiopathic Pulmonary Fibrosis: A Model for “Active” Disease. *PLoS One* 2013;8(4):e59348.

39. Ferrari D et al. The $P2X_7$ Receptor: A Key Player in IL-1 Processing and Release. *The Journal of Immunology* 2006;176(7):3877–3883.

40. Laurence A et al. Interleukin-2 signaling via STAT5 constrains T helper 17 cell generation.. *Immunity* 2007;26(3):371–81.

41. Ishida Y, Kondo T, Takayasu T, Iwakura Y, Mukaida N. The essential involvement of cross-talk between IFN-gamma and TGF-beta in the skin wound-healing process.. *J Immunol* 2004;172(3):1848–55.

42. Park I-K, Letterio JJ, Gorham JD. TGF-beta 1 inhibition of IFN-gamma-induced signaling and Th1 gene expression in CD4+ T cells is Smad3 independent but MAP kinase dependent.. *Mol Immunol* 2007;44(13):3283–90.

43. Misharin A v et al. Monocyte-derived alveolar macrophages drive lung fibrosis and persist in the lung over the life span.. *J Exp Med* 2017;214(8):2387–2404.

44. McCubbrey AL et al. Deletion of c-FLIP from CD11bhi Macrophages Prevents Development of Bleomycin-induced Lung Fibrosis.. *Am J Respir Cell Mol Biol* 2018;58(1):66–78.

45. Gibbons MA et al. Ly6Chi monocytes direct alternatively activated profibrotic macrophage regulation of lung fibrosis.. *Am J Respir Crit Care Med* 2011;184(5):569–81.

46. Kreuter M et al. Monocyte Count as a Prognostic Biomarker in Patients with Idiopathic Pulmonary Fibrosis.. *Am J Respir Crit Care Med* 2021;204(1):74–81.

47. Scott MKD et al. Increased monocyte count as a cellular biomarker for poor outcomes in fibrotic diseases: a retrospective, multicentre cohort study.. *Lancet Respir Med* 2019;7(6):497–508.

48. Achaiah A et al. Monocyte and neutrophil levels are potentially linked to progression to IPF for patients with indeterminate UIP CT pattern. *BMJ Open Respir Res* 2021;8(1):e000899.

49. Liu Y-Z et al. Proportions of resting memory T cells and monocytes in blood have prognostic significance in idiopathic pulmonary fibrosis. *Genomics* 2019;111(6):1343–1350.

50. Morimoto Y et al. Amphiregulin-Producing Pathogenic Memory T Helper 2 Cells Instruct Eosinophils to Secrete Osteopontin and Facilitate Airway Fibrosis.. *Immunity* 2018;49(1):134-150.e6.

51. Jenkins RG et al. An Official American Thoracic Society Workshop Report: Use of Animal Models for the Preclinical Assessment of Potential Therapies for Pulmonary Fibrosis. *Am J Respir Cell Mol Biol* 2017;56(5):667–679.

52. Hübner R-H et al. Standardized quantification of pulmonary fibrosis in histological samples. *Biotechniques* 2008;44(4):507–517.

53. di Virgilio F, Vuerich M. Purinergic signaling in the immune system.. *Auton Neurosci* 2015;191:117–23.

54. Sáez PJ et al. ATP promotes the fast migration of dendritic cells through the activity of pannexin 1 channels and P2X7 receptors.. *Sci Signal* 2017;10(506). doi:10.1126/scisignal.aah7107

55. Iwai Y et al. An IFN-gamma-IL-18 signaling loop accelerates memory CD8+ T cell proliferation.. *PLoS One* 2008;3(6):e2404.

56. Penton-Rol G et al. Selective inhibition of expression of the chemokine receptor CCR2 in human monocytes by IFN-gamma.. *J Immunol* 1998;160(8):3869–73.

57. de Bruin AM et al. Eosinophil differentiation in the bone marrow is inhibited by T cell-derived IFN-gamma.. *Blood* 2010;116(14):2559–69.

58. Iwamoto I, Nakajima H, Endo H, Yoshida S. Interferon gamma regulates antigen-induced eosinophil recruitment into the mouse airways by inhibiting the infiltration of CD4+ T cells.. *J Exp Med* 1993;177(2):573–6.

59. Raghu G et al. An Official ATS/ERS/JRS/ALAT Clinical Practice Guideline: Treatment of Idiopathic Pulmonary Fibrosis. An Update of the 2011 Clinical Practice Guideline.. *Am J Respir Crit Care Med* 2015;192(2):e3-19.

60. Lasithiotaki I et al. NLRP3/Caspase-1 inflammasome activation is decreased in alveolar macrophages in patients with lung cancer.. *PLoS One* 2018;13(10):e0205242.

61. Lasithiotaki I et al. NLRP3 inflammasome expression in idiopathic pulmonary fibrosis and rheumatoid lung.. *Eur Respir J* 2016;47(3):910–8.

62. Patel AS et al. Autophagy in idiopathic pulmonary fibrosis.. *PLoS One* 2012;7(7):e41394.

63. Young CNJ et al. A novel mechanism of autophagic cell death in dystrophic muscle regulated by P2RX7 receptor large-pore formation and HSP90.. *Autophagy* 2015;11(1):113–30.

64. Dupont N et al. Autophagy-based unconventional secretory pathway for extracellular delivery of IL-1β.. *EMBO J* 2011;30(23):4701–11.

65. Artlett CM et al. The inflammasome activating caspase 1 mediates fibrosis and myofibroblast differentiation in systemic sclerosis.. *Arthritis Rheum* 2011;63(11):3563–74.

66. Cameron LA et al. Airway epithelium expresses interleukin-18.. *Eur Respir J* 1999;14(3):553–9.

67. Watanabe A et al. Inflammasome-mediated regulation of hepatic stellate cells.. *Am J Physiol Gastrointest Liver Physiol* 2009;296(6):G1248-57.

68. Pinar AA, Yuferov A, Gaspari TA, Samuel CS. Relaxin Can Mediate Its Anti-Fibrotic Effects by Targeting the Myofibroblast NLRP3 Inflammasome at the Level of Caspase-1.. *Front Pharmacol* 2020;11:1201.

69. Khalil N et al. Increased production and immunohistochemical localization of transforming growth factor-beta in idiopathic pulmonary fibrosis.. *Am J Respir Cell Mol Biol* 1991;5(2):155–62.

70. Koutoulaki A, Langley M, Sloan AJ, Aeschlimann D, Wei X-Q. TNFalpha and TGF-beta1 influence IL-18-induced IFNgamma production through regulation of IL-18 receptor and T-bet expression.. *Cytokine* 2010;49(2):177–84.

71. Sharawy MH, Serrya MS. Pirfenidone attenuates gentamicin-induced acute kidney injury by inhibiting inflammasome-dependent NLRP3 pathway in rats.. *Life Sci* 2020;260:118454.

72. Oku H et al. Antifibrotic action of pirfenidone and prednisolone: different effects on pulmonary cytokines and growth factors in bleomycin-induced murine pulmonary fibrosis.. *Eur J Pharmacol* 2008;590(1–3):400–8.

73. Mavrogiannis E et al. Pirfenidone ameliorates pulmonary arterial pressure and neointimal remodeling in experimental pulmonary arterial hypertension by suppressing NLRP3 inflammasome activation.. *Pulm Circ* 2022;12(3):e12101.

74. Spagnolo P et al. Idiopathic pulmonary fibrosis: Disease mechanisms and drug development. *Pharmacol Ther* 2021;222:107798.

75. Raghu G et al. Diagnosis of Idiopathic Pulmonary Fibrosis. An Official ATS/ERS/JRS/ALAT Clinical Practice Guideline. *Am J Respir Crit Care Med* 2018;198(5):e44–e68.

76. Migliorini P et al. Serum and urinary levels of IL-18 and its inhibitor IL-18BP in systemic lupus erythematosus.. *Eur Cytokine Netw* 2010;21(4):264–71.

77. Schindelin J et al. Fiji: an open-source platform for biological-image analysis. *Nat Methods* 2012;9(7):676–682.

Figure legends

Figure 1 : The P2RX7/IL-18/IFN-γ pathway is downregulated in IPF

(A) Heatmap of mRNA expression of P2RX7 in control and IPF patients with a cluster of fibrosis-associated genes. Raw p-values are shown (Limma). **(B)** mRNA expression of *P2RX7, IL18, IL18R1, IL18RAP* and *IFNG* between control and IPF patients. Each point represents one patient. Two-tailed unpaired t-test with Welch's correction, ***$p < 0.001$, ****$p < 0.0001$. **(C)** Gene set enrichment analysis (GSEA) plot associating P2RX7 mRNA levels from IPF patients with three immunological signatures. The green line represents the enrichment score and the black lines the specific signature-associated genes. NES: Normalized enrichment score, FDR: False discovery rate. Pearson's correlation test.

Figure 2 : Activation of P2RX7 with HEI3090 inhibits lung fibrosis progression

(A) Experimental design. WT mice were given 2.5 U/kg of bleomycin by i.n. route and treated daily i.p. with 1.5 mg/kg of HEI3090 or Vehicle. **(B)** Representative images of lung sections at day 14 after treatment stained with H&E and Sirius Red, Scale bar= 100 µm. **(C)** Fibrosis score assessed by the Ashcroft method. **(D)** Collagen levels in whole lung of mice assessed on Sirius Red-polarized images. **(E)** Lung weight of naïve and BLM-induced mice at day 14 **(F)** IL-18 levels in sera of BLM-induced mice at day 14 **(G)** Contour plot of IFN-γ and IL-17A producing T cells ($CD3^+NK1.1^-$) (left) and ratio of IFN-γ over IL-17A in T cells ($CD3^+NK1.1^-$) (right). Each point represents one mouse, two-tailed Mann-Whitney test, p values: *$p < 0.05$, **$p < 0.01$, ****$p < 0.0001$. WT: Wildtype, BLM: bleomycin, i.p.: intraperitoneal, i.n.: intranasal, H&E: hematoxylin&eosin

Figure 3: The P2RX7/NLRP3/IL-18 pathway in immune cells is required for HEI3090's antifibrotic effect

(A) Experimental design. *p2rx7*$^{-/-}$ mice were given 3.10^6 WT*, nlrp3*$^{-/-}$ or *il18*$^{-/-}$ splenocytes i.v. one day prior to BLM delivery (i.n. 2.5 U/kg). Mice were treated daily i.p. with 1.5 mg/kg HEI3090 or vehicle for

14 days. **(B,D,F)** Representative images of lung sections at day 14 after treatment stained with H&E and Sirius Red, scale bar= 100 µm. Fibrosis score assessed by the Ashcroft method of adoptive transfer of WT splenocytes, **(E)** *nlrp3*$^{-/-}$ splenocytes and **(G)** *il18*$^{-/-}$ splenocytes. Each point represents one mouse, two-tailed Mann-Whitney test, *$p < 0.05$. WT: Wildtype, BLM: bleomycin, i.p.: intraperitoneal, i.n.: intranasal, i.v.: intravenous, H&E: hematoxylin&eosin

Figure 4 : HEI3090 enhances IL-18 release and favors an anti-fibrotic immune signature in the lungs

WT mice were given 2.5 U/kg of bleomycin by i.n. route and treated daily i.p. with 1.5 mg/kg of HEI3090 or Vehicle. Lungs were analyzed by flow cytometry at day 14. **(A)** Percentage and GMFI of IL-17A^{+} cells of CD4^{+} T cells (CD3^{+}CD4^{+}NK1.1^{-}). **(B)** Percentage and GMFI of TGFβ in CD45^{+} cells. **(C)** Dotplot showing lung inflammatory monocytes, gated on lineage^{-}CD11c^{-}CD11b^{+} cells (left) and percentage of lung inflammatory monocytes (Ly6C^{high}Ly6G^{-}) (right) **(D)** Percentage of alveolar macrophages (CD11c^{+}SiglecF^{+}) **(E)** Percentage of lung eosinophils (CD11b^{+}SiglecF^{+}CD11c^{-}). Each point represents one mouse, data represented as violin plots or mean±SEM, two-tailed Mann-Whitney test, *$p < 0.05$, **$p < 0.01$. GMFI: geometric mean fluorescence intensity. i.n.: intranasal, i.p.: intraperitoneal

Figure 5: IL-18 bioavailability is a predictive biomarker for IPF progression and patient survival

(A) Levels of free IL-18 and the IL-18/IL-18BP complex in plasma of healthy persons and IPF patients. Cut-off for free IL-18 and IL-18/IL-18BP complex was the median of values of IPF patients. Each point represents one patient, mean ± SEM. Two-tailed unpaired t-test with Welch's correction (B) Survival curve of IPF patients according to their levels of plasmatic free IL-18 or complexed IL-18. Log-rank Mantel Cox test. **$p < 0.01$, ***$p<0.001$. IL-18BP: IL-18Binding Protein, IPF: idiopathic pulmonary fibrosis

Table 1. Clinical characteristics of IPF patients

Clinical characteristics	IPF Patients	Progressive disease	Non Progressive disease	Control
Number n=	18	4	14	9
Age (years, mean ± SD)	73.3 ± 5.54	70.75 ± 6.18	74.07 ± 5.35	41.29 ± 16.54
Gender				
Male n=	15	3	12	4
Female n=	3	1	2	5
Smoking history				
Non smoker n=	6	1	5	
Active smoker n=	2	2	8	
Past smoker n=	10	1	1	
Pack-years (mean ± SD)	22.33 ± 17.65	25.33 ± 4.04	21.33 ± 20.49	
Antifibrotic treatment				
Pirfenidone n=	5	1	4	
Nintedanib n=	9	3	6	
Other n=	1	0	1	
None n=	3	0	3	
Pulmonary function test				
FVC (% mean ± SD)	78.89 ± 18.8	59.25 ± 12.45	84.5 ± 16.55	
DLCO (% mean ± SD)	60.28 ± 18.59	41.75 ± 13.25	65.57 ± 16.6	
GAP stage				
Stage 1 n=	10	0	10	
Stage 2 n=	6	3	3	
Stage 3 n=	2	1	1	

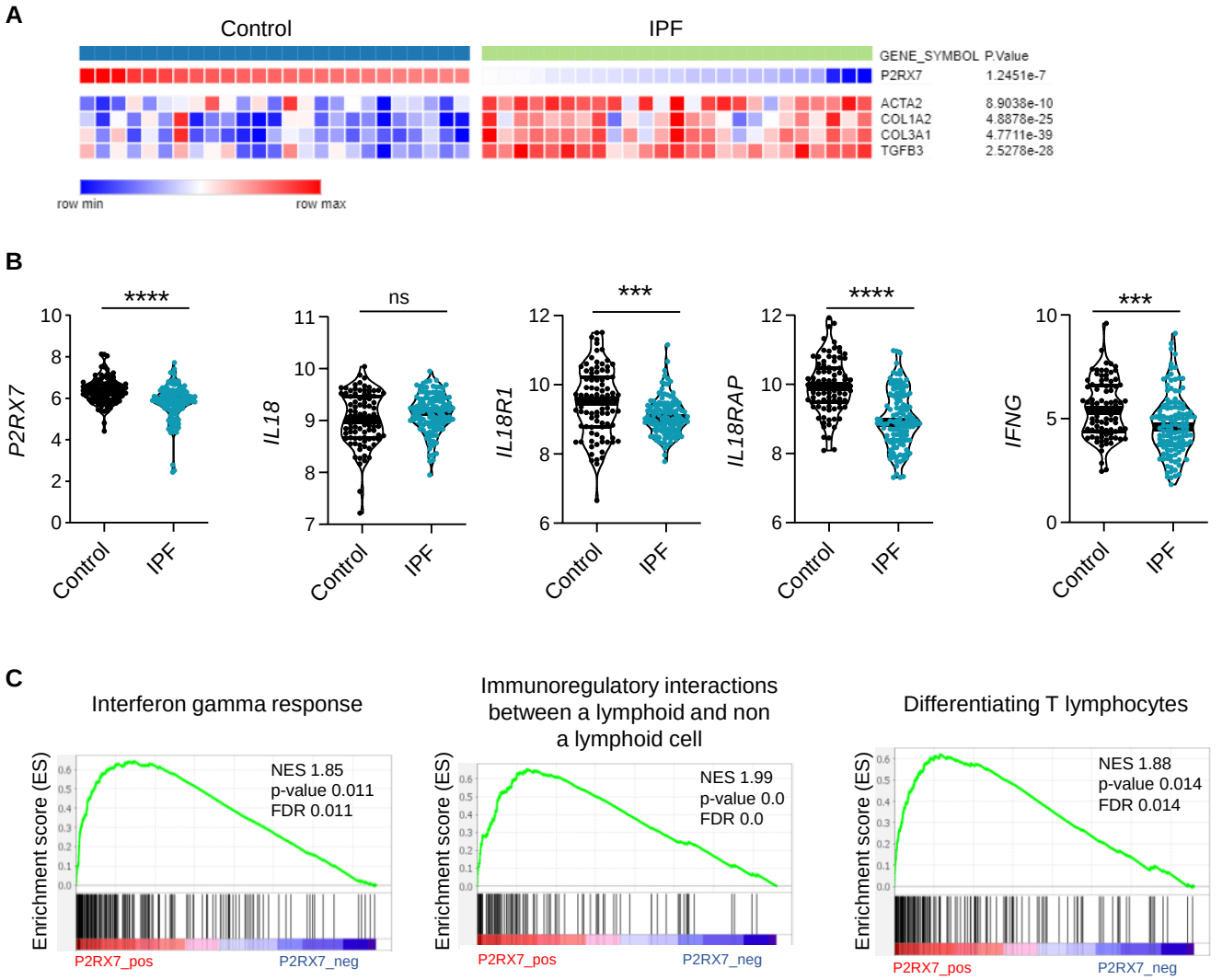

Figure 1 : The P2RX7/IL-18/IFN-γ pathway is downregulated in IPF

(A) Heatmap of mRNA expression of P2RX7 in control and IPF patients with a cluster of fibrosis-associated genes. Raw p-values are shown (Limma). **(B)** mRNA expression of *P2RX7, IL18, IL18R1, IL18RAP* and *IFNG* between control and IPF patients. Each point represents one patient. Two-tailed unpaired t-test with Welch's correction, ***$p < 0.001$, ****$p < 0.0001$. **(C)** Gene set enrichment analysis (GSEA) plot associating P2RX7 mRNA levels from IPF patients with three immunological signatures. The green line represents the enrichment score and the black lines the specific signature-associated genes. NES: Normalized enrichment score, FDR: False discovery rate. Pearson's correlation test.

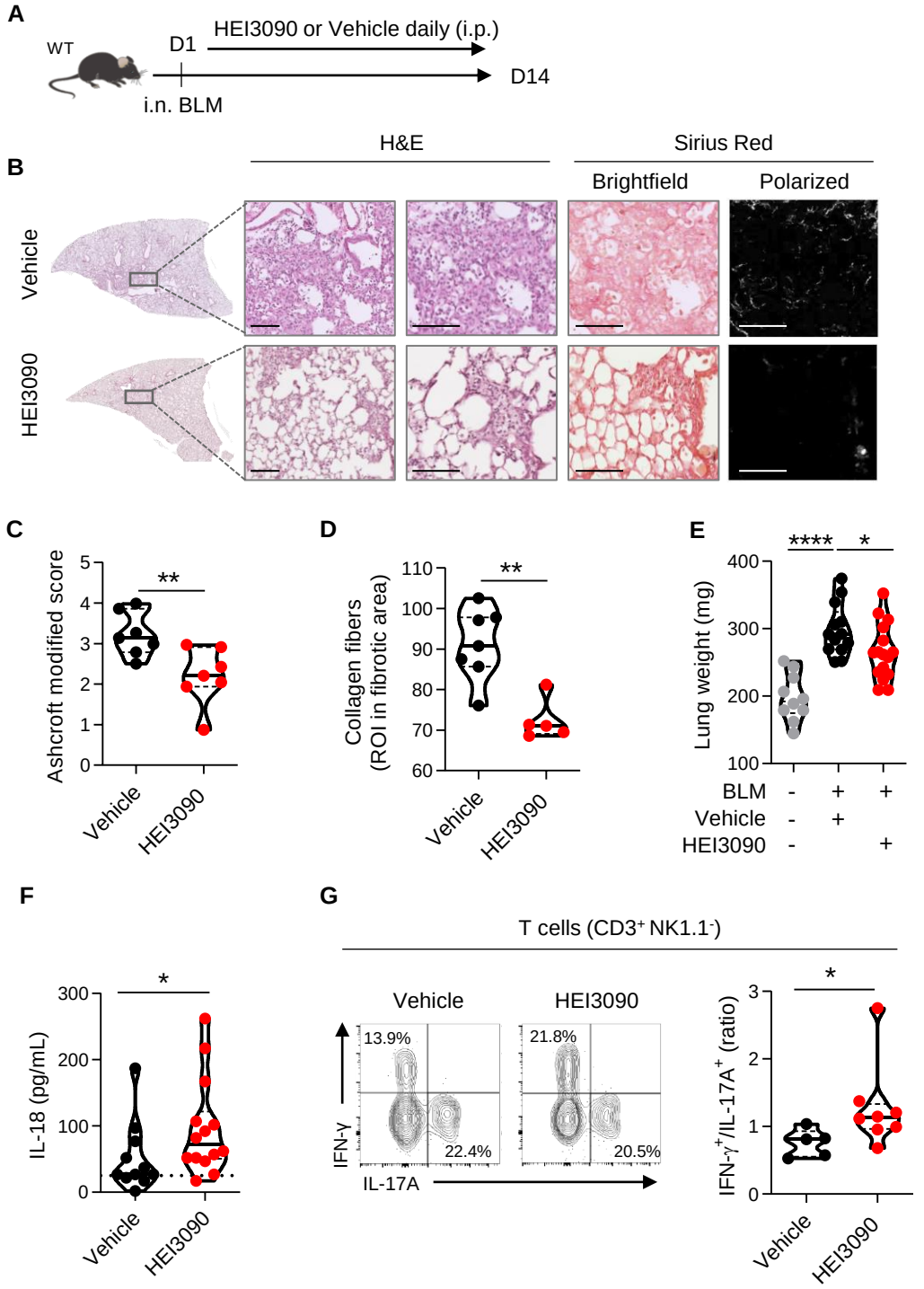

Figure 2 : Activation of P2RX7 with HEI3090 inhibits lung fibrosis progression

(A) Experimental design. WT mice were given 2.5 U/kg of bleomycin by i.n. route and treated daily i.p. with 1.5 mg/kg of HEI3090 or Vehicle. **(B)** Representative images of lung sections at day 14 after treatment stained with H&E and Sirius Red, Scale bar= 100 µm. **(C)** Fibrosis score assessed by the Ashcroft method. **(D)** Collagen levels in whole lung of mice assessed on Sirius Red-polarized images. **(E)** Lung weight of naïve and BLM-induced mice at day 14 **(F)** IL-18 levels in sera of BLM-induced mice at day 14 **(G)** Contour plot of IFN-γ and IL-17A producing T cells ($CD3^+NK1.1^-$) (left) and ratio of IFN-γ over IL-17A in T cells ($CD3^+NK1.1^-$) (right). Each point represents one mouse, two-tailed Mann-Whitney test, p values: *$p < 0.05$, **$p < 0.01$, ****$p < 0.0001$. WT: Wildtype, BLM: bleomycin, i.p.: intraperitoneal, i.n.: intranasal, H&E: hematoxylin&eosin

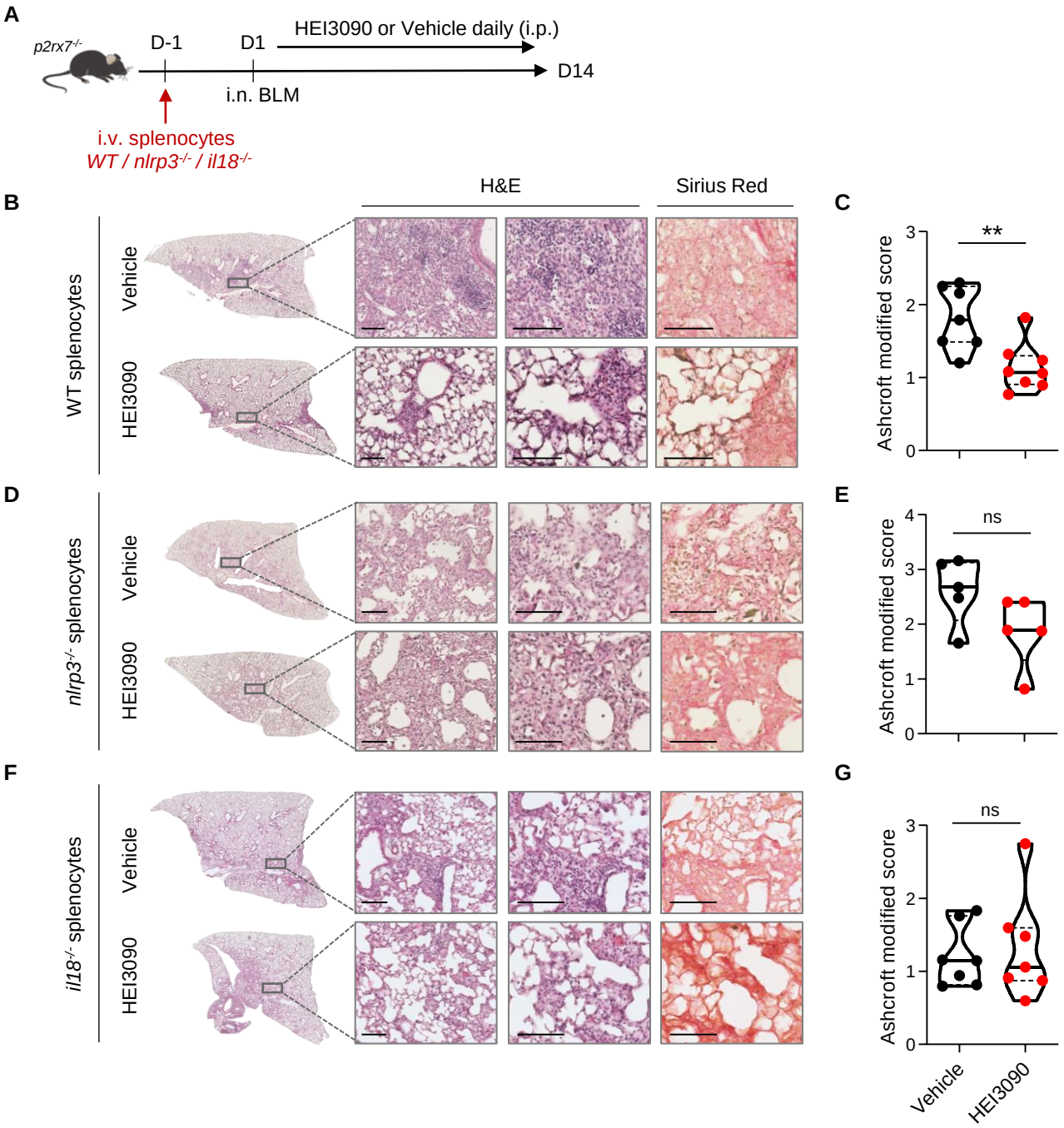

Figure 3: The P2RX7/NLRP3/IL-18 pathway in immune cells is required for HEI3090's antifibrotic effect

(A) Experimental design. *p2rx7*$^{-/-}$ mice were given 3.10^6 WT, *nlrp3*$^{-/-}$ or *il18*$^{-/-}$ splenocytes i.v. one day prior to BLM delivery (i.n. 2.5 U/kg). Mice were treated daily i.p. with 1.5 mg/kg HEI3090 or vehicle for 14 days. **(B,D,F)** Representative images of lung sections at day 14 after treatment stained with H&E and Sirius Red, scale bar= 100 µm. Fibrosis score assessed by the Ashcroft method of adoptive transfer of WT splenocytes, **(E)** *nlrp3*$^{-/-}$ splenocytes and **(G)** *il18*$^{-/-}$ splenocytes. Each point represents one mouse, two-tailed Mann-Whitney test, *$p < 0.05$. WT: Wildtype, BLM: bleomycin, i.p.: intraperitoneal, i.n.: intranasal, i.v.: intravenous, H&E: hematoxylin&eosin

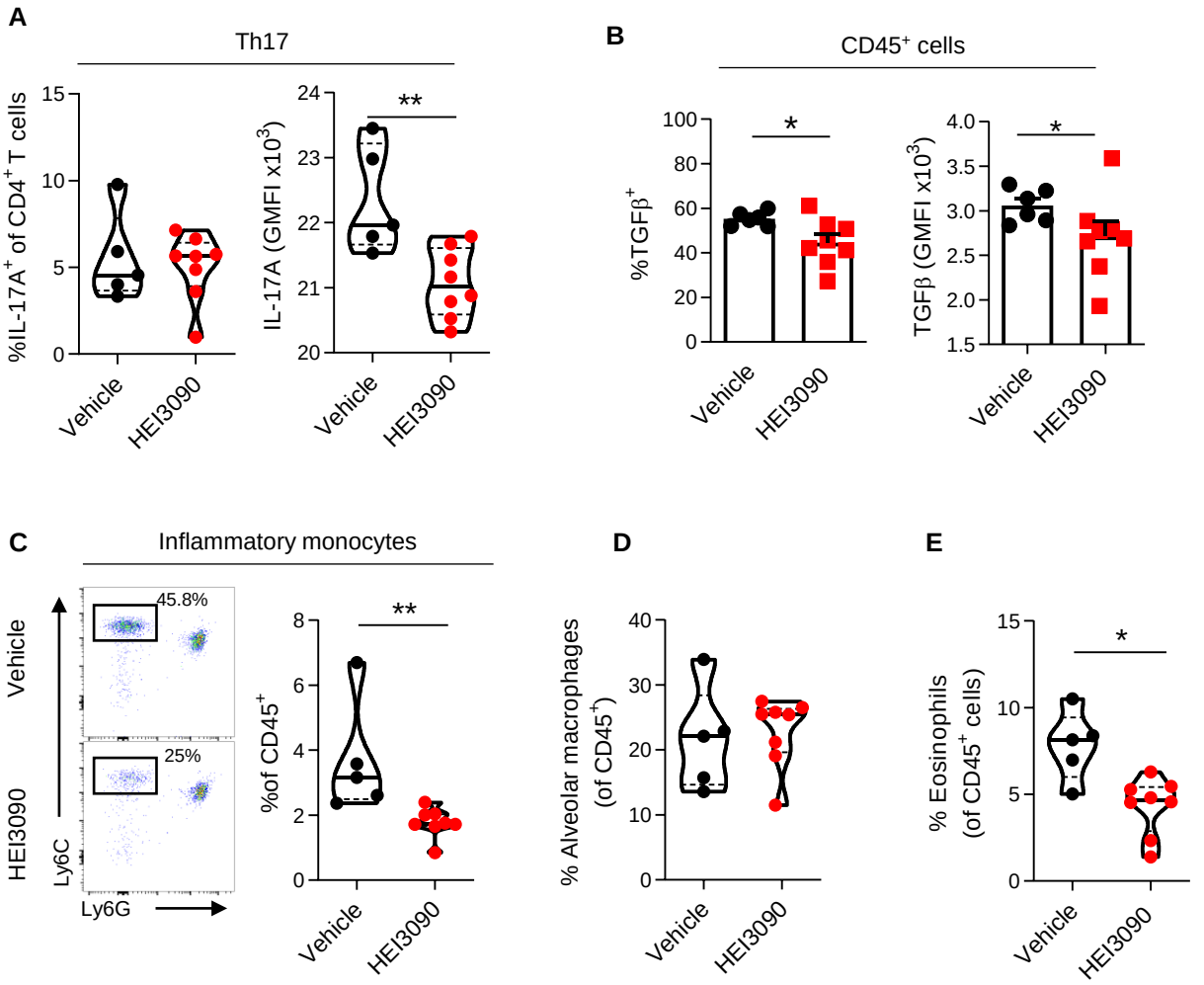

Figure 4 : HEI3090 enhances IL-18 release and favors an anti-fibrotic immune signature in the lungs

WT mice were given 2.5 U/kg of bleomycin by i.n. route and treated daily i.p. with 1.5 mg/kg of HEI3090 or Vehicle. Lungs were analyzed by flow cytometry at day 14. **(A)** Percentage and GMFI of IL-17A$^+$ cells of CD4$^+$ T cells (CD3$^+$CD4$^+$NK1.1$^-$). **(B)** Percentage and GMFI of TGFβ in CD45$^+$ cells. **(C)** Dotplot showing lung inflammatory monocytes, gated on lineage$^-$ CD11c$^-$CD11b$^+$ cells (left) and percentage of lung inflammatory monocytes (Ly6C^{high}Ly6G$^-$) (right) **(D)** Percentage of alveolar macrophages (CD11c$^+$SiglecF$^+$) **(E)** Percentage of lung eosinophils (CD11b$^+$SiglecF$^+$CD11c$^-$). Each point represents one mouse, data represented as violin plots or mean±SEM, two-tailed Mann-Whitney test, *$p < 0.05$, **$p < 0.01$. GMFI: geometric mean fluorescence intensity. i.n.: intranasal, i.p.: intraperitoneal

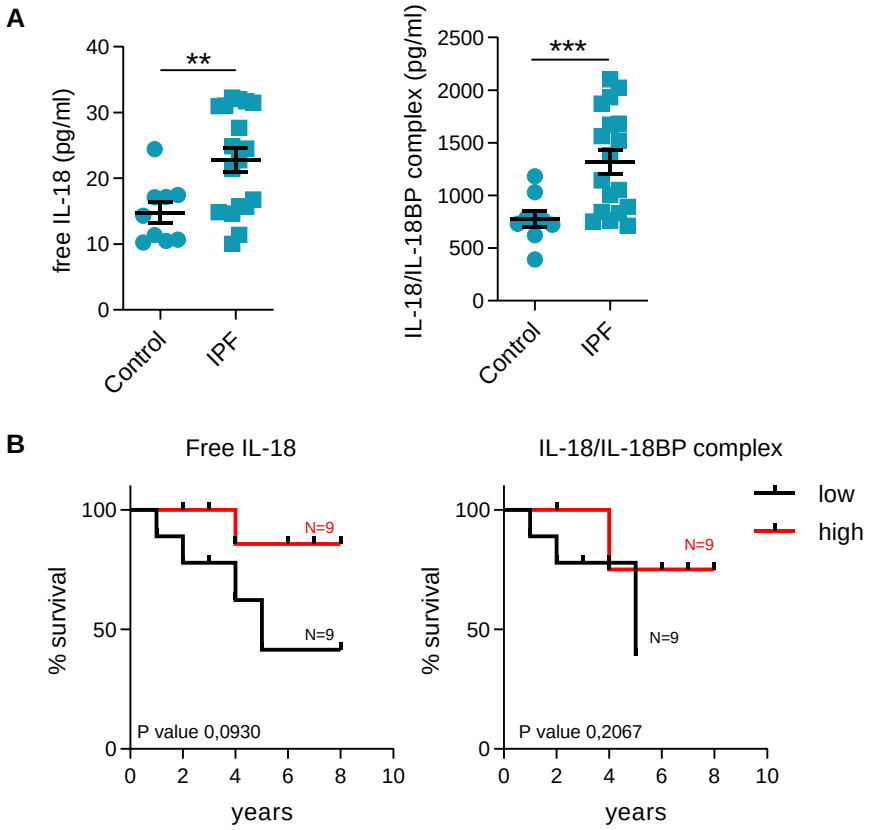

Figure 5: IL-18 bioavailability is a predictive biomarker for IPF progression and patient survival

(A) Levels of free IL-18 and the IL-18/IL-18BP complex in plasma of healthy persons and IPF patients. Cut-off for free IL-18 and IL-18/IL-18BP complex was the median of values of IPF patients. Each point represents one patient, mean ± SEM. Two-tailed unpaired t-test with Welch's correction (B) Survival curve of IPF patients according to their levels of plasmatic free IL-18 or complexed IL-18. Log-rank Mantel Cox test. **$p < 0.01$, ***$p<0.001$. IL-18BP: IL-18Binding Protein, IPF: idiopathic pulmonary fibrosis